

## **Computer Microvision for MEMS**

### **Academic and Research Staff**

Professor Dennis M. Freeman, Professor Berthold K. Horn, Michael B. McIlrath

### **Research Affiliates**

Dr. C. Cameron Abnet, Daniel Feldkhun, Abraham McAllister, Dr. Michael S. Mermelstein

### **Graduate Students**

Salil P. Desai, Stanley S. Hong, Jekwan Ryu

### **Support Staff**

Chris Morocco, Janice Balzer

### **Sponsors**

Defense Advanced Research Projects Agency Grant F30602-97-2-0106  
Defense Advanced Research Projects Agency Grant N66001-00-1-8908  
Center for National Research Initiatives Matisse Project  
W.M. Keck Foundation Career Development Professorship (Freeman)

## **1. Computer Microvision for MEMS**

### **Academic and Research Staff**

Professor Dennis M. Freeman, Michael B. McIlrath

### **Research Affiliates**

Dr. C. Cameron Abnet, Daniel Feldkhun, Abraham McAllister, Dr. Michael S. Mermelstein

### **Graduate Students**

Salil P. Desai

### **Sponsors**

Defense Advanced Research Projects Agency Grant F30602-97-2-0106  
Center for National Research Initiatives Matisse Project  
W.M. Keck Foundation Career Development Professorship (Freeman)

### **Introduction**

Microelectromechanical Systems (MEMS) are fabricated using batch techniques that are similar to those used to fabricate microelectronic devices. Unlike electronics, however, simple methods for testing and characterizing internal failure modes of micromechanical devices do not exist. The major goal of this project is to develop inexpensive and reliable tools for in situ visualization of the motions of internal structures in MEMS by combining light microscopy, video imaging, and machine vision.

We have previously demonstrated in situ measurements of 3D motions of MEMS using the combination of brightfield microscopy and Mirau interferometry. The Mirau interferometric video system combines the superior out-of-plane resolution of interference methods with the superior in-plane resolution of brightfield computer microvision to achieve three-dimensional measurements with nanometer resolution in all 3 directions.

**Six Degree-of-Freedom Motion Measurements**

The Mirau interferometric system combines brightfield and interferometric measurements, allowing for high resolution 6 degree-of-freedom motion measurements. Brightfield images provide motion information for the 3 in-plane degrees-of-freedom, (1) translation in  $x$ , (2) translation in  $y$ , and (3) rotation about  $z$ . However, the lower out-of-plane resolution of the brightfield computer microvision system results in decreased measurement resolution for out-of-plane degrees of freedom. Interferometric techniques provide higher out-of-plane resolution and consequently higher motion measurement resolution for the 3 out-of-plane degrees-of-freedom, (1) translation in  $z$ , (2) rotation about  $x$ , and (3) rotation about  $y$ .

To demonstrate 6 degree-of-freedom motion measurement, a surface micromachined lateral resonator (fabricated with MUMPs, Cronos Integrated Microsystems, USA) was electrically stimulated with a sinusoidal voltage (10Vp-p AC plus 50V DC bias) applied to one of the comb drives and the shuttle mass was connected to ground. The system was placed on a vibration isolation table and in an enclosure to minimize the effects of external vibrations and air currents.

Stroboscopic illumination was used to take stop-action brightfield images (Figure 1a) and stop-action interferograms (Figure 1b) at multiple phases of periodically driven motions of the MEMS device under test. Illumination was generated using an array of seven LEDs (C505-CB290-E1000, Cree Research Inc., USA). The fast optical rise time of the LEDs (30ns) allows stop-action motion analysis at frequencies up to tens of MHz. The optical bandwidth (50nm centered at  $\lambda = 505\text{nm}$ ) produces light with a coherence length of approximately  $15\mu\text{m}$ . Thus, interferometric

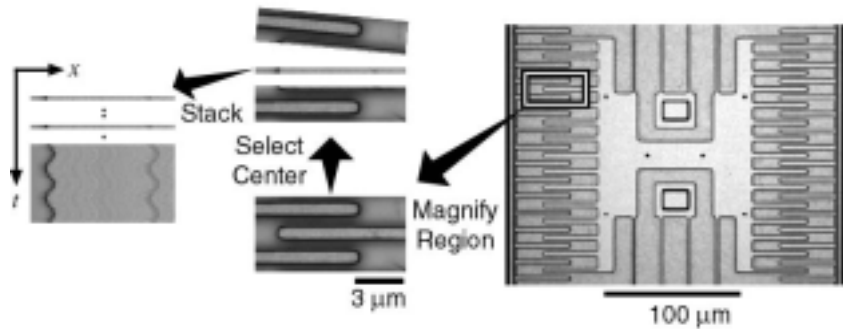


Figure 1a: Motion measurement from brightfield images

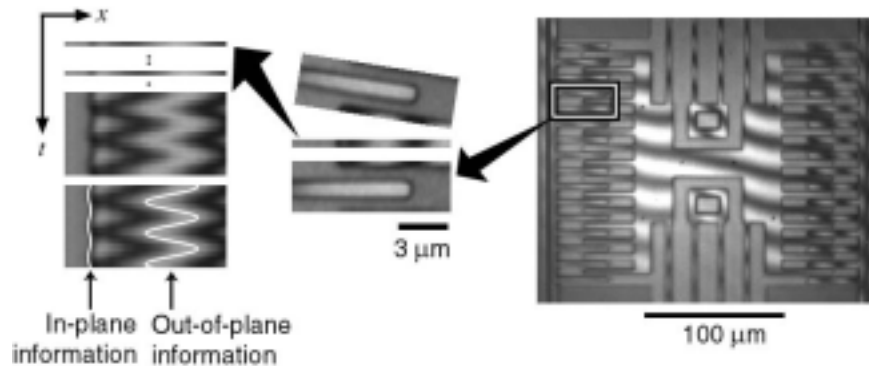


Figure 1b: Motion measurement from interferometric images

data can be obtained from structures with heights within a  $7\mu\text{m}$  range. Brightfield images and interferograms were obtained at 8 evenly spaced phases of motion and recorded with a CCD camera (Pulnix 1010, Pulnix Inc., USA). Interferograms at nine planes of focus (separated by 30nm) and one brightfield image (at the plane of best focus) were obtained for 8 stimulus phases at each of 33 frequencies (from 1kHz to 50kHz).

Brightfield images were analyzed to determine displacements in the  $x$ -direction, displacements in the  $y$ -direction and in-plane rotations (about the  $z$ -direction). These results are plotted as time waveforms for one cycle of the stimulus (Figure 2, left panel). Displacements in the  $x$ -direction are approximately sinusoidal. The estimated amplitude and angle are 128.9 nm and  $-14.2$  degrees, respectively. The other in-plane measurements (Figure 2, left panel) are on the order of the noise floor of the measurement.

Interferometric images were analyzed to determine displacements in the  $z$ -direction, rotations about the  $x$ -direction and rotations about the  $y$ -direction. These results are plotted as time waveforms for one cycle of the stimulus (Figure 2, right panel). Displacements in the  $z$ -direction and rotations about the  $y$ -direction are approximately sinusoidal. The estimated amplitude and angle for displacement in the  $z$ -direction are 37.8 nm and  $-39.7$  degrees, respectively. The estimated amplitude and angle for rotation about the  $y$ -direction are 62.3 millidegrees and  $-31.1$  degrees, respectively. Rotation about the  $x$ -direction (Figure 2, right panel) is on the order of the noise floor.

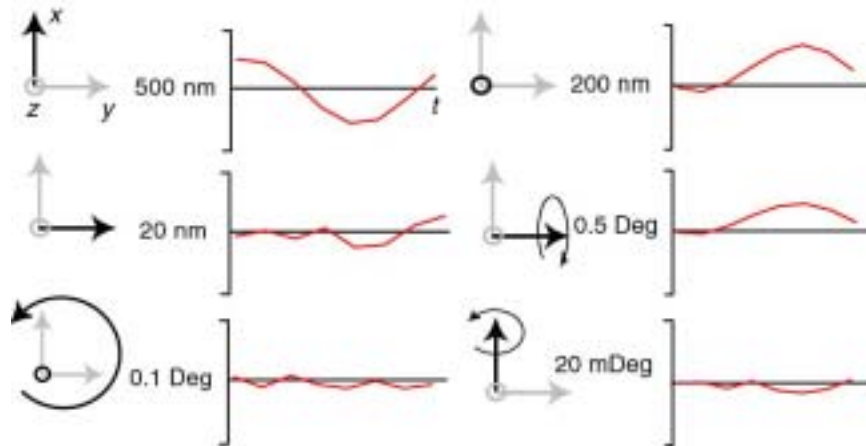


Figure 2: Time waveforms of motion for 3 in-plane degrees-of-freedom (left panel), and 3 out-of-plane degrees-of-freedom (right panel)

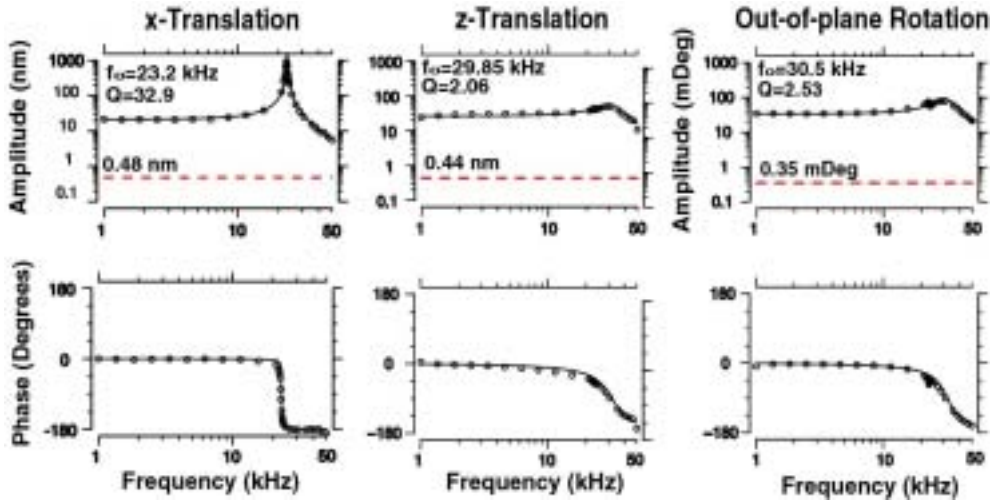


Figure 3: Magnitude and phase of frequency response for translation in x (left), translation in z (center), and rotation about y (right)

Similar results were obtained for 33 frequencies from 1 kHz to 50 kHz. Amplitudes and angles for displacements in the x-direction are illustrated by the circles in Figure 3 (left panel). These measurements were fit with a second-order resonance curve (indicated by the solid line), which exhibited a sharp resonant peak ( $Q = 32.95$ ) at 23.2 kHz. The phase response exhibited a sharp roll-off at resonance. The noise floor was measured as 0.48 nm (indicated by the dashed line).

Amplitudes and angles for displacements in the z-direction are shown in Figure 3 (center panel). These measurements were fit with a second-order resonance curve with resonance frequency of 29.85 kHz and  $Q = 2.06$ . The noise floor of the measurement was 0.44 nm.

Amplitudes and angles for rotations about the y-direction are shown in Figure 3 (right panel). These measurements were fit with a second-order resonance with resonance frequency of 30.55 kHz and  $Q = 2.53$ . The noise floor of the measurement was 0.35 millidegree.

### Dynamic Profilometry

The Mirau interferometric system allows for measurement of both static and dynamic profiles of all structures within the field of view. Using phase-shifting interferometry, the out-of-plane position of each individual pixel in an interferometric image can be determined, independent of all other pixels. This provides high-resolution static profiling capability. Using this technique in combination with stroboscopic illumination, profiles can be reconstructed at different temporal phases of the stimulus waveform, thereby enabling dynamic profilometry.

Electrostatically deformable surface micromachined diffraction gratings (designed at the University at Albany, State University of New York) were used to demonstrate the dynamic profiling capability of the system. Deformations were stimulated by applying a sinusoidal waveform (20V peak-to-peak AC plus 30V DC bias) to the movable grating with the underlying electrode grounded.

Deformations of the diffraction grating were determined from stroboscopic interferograms at 20 z positions (separated by 50 nm) for 8 stimulus phases at a frequency of 1 kHz. Each pixel in the sequence collects an intensity that varies sinusoidally with z. The amplitude of this sinusoidal variation is proportional to the reflectivity of the device. The phase of the sinusoidal intensity variation encodes the relative out-of-plane position of the device. For each pixel, brightness

variations as a function of  $z$  were fit with a sinusoid using a least-squares technique. Out-of-plane positions were determined from the phase of the best fitting sinusoid.

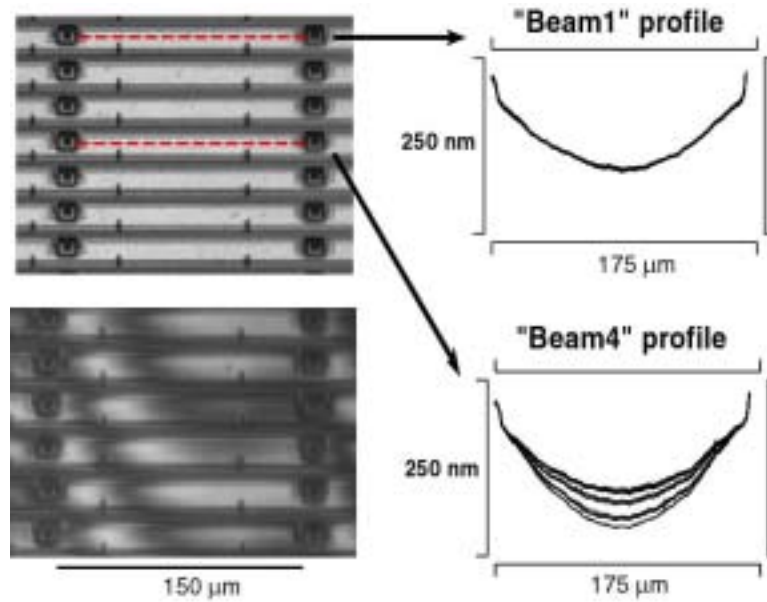


Figure 4: Dynamic profilometry results for surface-micromachined diffraction gratings

Out-of-plane positions along one grating are shown for 8 phases in Figure 4. For all phases, the profiles are bowed and the displacements of the center point of the grating are approximately 100 nm closer to the substrate than are the anchored portions of the grating. The bowing changes periodically with the stimulus. The amplitude and angle of the displacements of the center of the grating are 26.6 nm and  $-4.2$  degrees, respectively. Not all gratings bowed identically. The top panel of Figure 4 shows results for a different grating that was not electrically stimulated and all 8 phases show the same curvature.

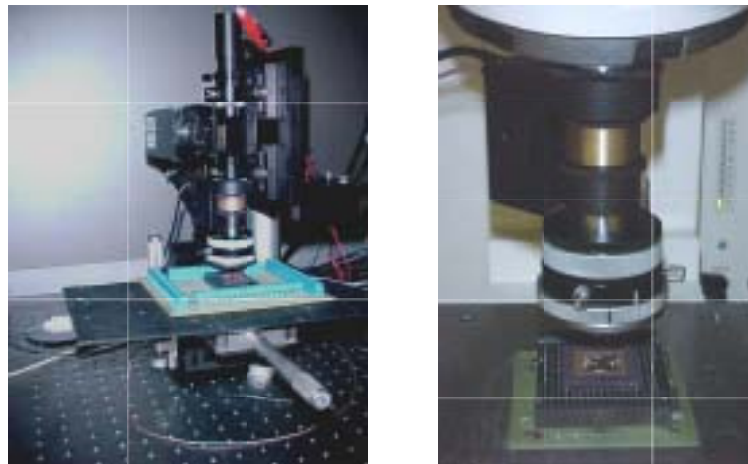


Figure 5: Photograph of benchtop Mirau interferometric system (left), and close-up picture of Mirau interferometric setup (right)

### **Benchtop Mirau Interferometric Computer Microvision System**

We have developed a benchtop system for Interferometric Computer Microvision (Figure 5). The benchtop system can be made optically more efficient than our systems based on commercial microscopes because we can customize the illumination for a single microscope for a single microscope objective (Zeiss' LD Epiplan 20X). The illumination systems in our commercial microscopes (Zeiss Axioplan 2) are designed to support Zeiss' entire line of objectives, whose magnifications range over more than two orders of magnitude. By customizing the illumination system, we have achieved more than an order of magnitude increase in light intensity from the same LED.

We have also identified a source of brighter LEDs. We have previously used LEDs from Nichia (NSPG500S) and Cree (C505-CB290-E1000), which can generate 3.5mW of continuous light. We have obtained a brighter LED from Luxeon Corporation (Star /C Batwing) that can generate 50mW of continuous light. The Luxeon LED will be integrated into our benchtop system.

### **High-Speed Imaging**

In the brightfield computer microvision system, stroboscopic illumination is accomplished by switching the current to the LED on and off with a high-speed transistor (ZVN3306A). Because the LEDs are fast, the shortest light pulse is limited in practice by the electronics driving the LED (~100ns). Hence, the brightfield system achieves a stroboscopic sampling rate of 10MHz.

To increase the stroboscopic sampling, a commercial laser diode driver (EL6259C, Elantec Semiconductor, Inc.) is used for pulsing the LEDs. These drivers have low output noise and extremely short rise/fall times (~1ns). This would result in an order of magnitude increase in the stroboscopic sampling rate, thereby enabling high-speed measurement.

By increasing the light output and light efficiency, and consequently the stroboscopic sampling rate of the imaging system, transient behavior of MEMS devices can be measured.

### **Publications**

#### **Conference Proceedings**

D.M. Freeman, "Computer Microvision for MEMS," invited paper, in *Material Science of Microelectromechanical Systems (MEMS) Devices II*, M. de Boer, A. Heuer, S. Jacobs, and E. Peeters, eds., Mat. Res. Soc. Symp. Proc., 605: 151-162 (2000).

S.P. Desai and D.M. Freeman, "Nanometer Resolution of Three-Dimensional Motion using Mirau Interferometric Optics," International iMEMS Workshop 2001, July 4-6, 2001, NUS, Singapore.

#### **Journal Articles, Published**

S.J. Timoner and D.M. Freeman, "Multi-Image Gradient-Based Algorithms for Motion Estimation," *Optical Engineering*, 40(9):2003-2016 (2001).

D.M. Freeman, "Measuring Motions of MEMS," *MRS Bulletin*, 26: 305-306, April 2001.

## **2. Synthetic Aperture Lithography**

### **Academic and Research Staff**

Professor Dennis M. Freeman, Professor Berthold K. P. Horn

### **Visiting Scientists and Research Affiliates**

Lightwave Instruments, LLC

### **Graduate Students**

Stanley S. Hong, Jekwan Ryu

### **Technical and Support Staff**

Janice L. Balzer

### **Sponsors**

Defense Advanced Research Projects Agency Grant N66001-00-1-8908

W.M. Keck Foundation Career Development Professorship (Freeman)

## **Introduction**

We have developed a novel approach to lensless and maskless projection of arbitrary optical patterns, which we call Synthetic Aperture Lithography (SAL). In traditional optical lithography, light from an illuminator passes through a mask and is focused by a lens to recreate the mask pattern on a wafer. The central idea in SAL is that the pattern of light that emerges from a lens will evolve into the same lithographic pattern regardless of how it was created. SAL replaces the lens, the mask, and the mask illuminator with a discrete set of controllable laser beams. By controlling the amplitudes and phases of the beams, lithographic patterns with diffraction-limited lateral resolution and essentially unlimited depth of focus can be projected.

## **Proof of Concept**

A prototype SAL projector was constructed using an acousto-optic deflector to break the beam of an argon ion laser into 29 spatially separated beams and to control the amplitude and phase of each. The beams were steered with an array of flat mirrors to illuminate a target region from 29 directions organized in a circular cone. Differences in beam amplitudes and phases introduced by the mirrors and acousto-optic deflector were calibrated and electronically compensated by changing the electrical signal driving the acousto-optic deflector. When the 29 beams were made to have equal amplitudes and equal phases at a target point, the resulting optical pattern was a "needle of light" oriented parallel to the axis of the cone of beams. The diameter of the needle was less than  $0.45 \lambda$ , and the length of the needle was greater than  $100 \lambda$ . The working distance was greater than 2 centimeters. Since the position of the needle can be controlled electronically by altering the relative phases of the beams, feedback can be used to compensate for unwanted substrate vibrations. To create useful lithographic structures, the needle can be scanned. Additionally, the method is not constrained to generating needles of light. More complex interference patterns may provide a more efficient set of basis functions for constructing lithographic patterns.